

Chapter 3

Loading of a MOT

3.1 Introduction

This chapter begins with a description of an experimental observation in our MOT. Fluorescence was measured from the cold cloud when the cooling beam was ramped in frequency and the repumper was kept locked at a fixed frequency. Certain puzzling features were observed, which are described. The process of loading and decay of MOT is examined and numerical simulations performed for the situation prevalent in a MOT, in order to determine the fluorescence expected. These give results remarkably close to experimental observations, enabling us to explain the experimentally observed features. Based on this a new method of determining lifetime of traps has been devised.

3.2 Experimental Details

The object of our study was the cold cloud of ^{85}Rb formed in a MOT. Usually the cloud is formed with the cooling and repumper beams locked. The typical detuning δ_c of the cooling beam is -1.5Γ . In our experiment, the repumper was kept locked at a detuning δ_r from the $F=3 \rightarrow F'=3$ transition. The cooling beam was then ramped in frequency, up and down from -125 MHz to 30 MHz (figure 3.1) about the cooling transition. For each fixed repumper frequency the ramp rate was changed from 1.55 MHz/sec (ramp period $T = 200$ s) to 155 MHz/sec (ramp period $T = 2$ s). The formation of the cloud and its decay was monitored by recording the fluorescence intensity from the centre of the MOT using a femtowatt detector.

The experiments were repeated for different detunings δ_R of the repumper laser, in the range +9.8 MHz to -9.8 MHz.

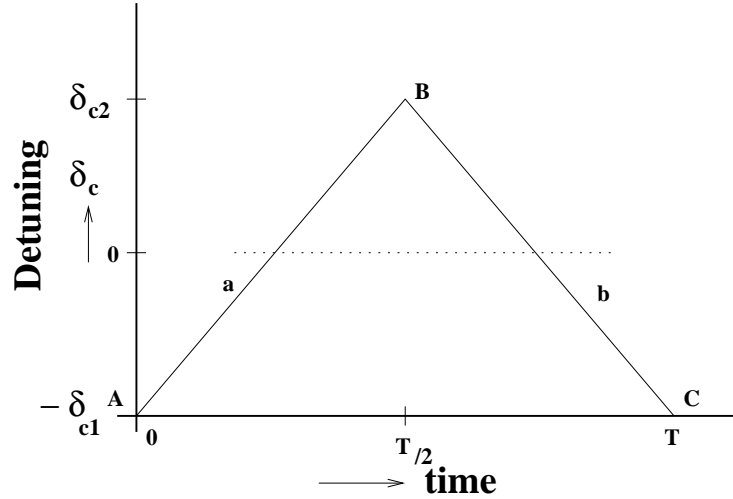


Figure 3.1: Variation of the detuning of the cooling laser with time between $-\delta_{c1}$ and δ_{c2} (schematic)

The schematic experimental set-up is shown in figure 3.2. The various beams were derived from two home-built external cavity diode lasers. Each gave two output beams, one of which went directly to the MOT, and the other to a saturated absorption set-up. The latter enabled us to actively lock the frequency of the laser. In cases when the frequency of the laser was being ramped, the saturation absorption provided a measure of the instantaneous frequency of the laser. In the case of the cooling laser, an AOM in the path of the saturation absorption set-up provided the MOT beam shifted in frequency higher by 82.2 MHz (see figure 3.3) from the value shown by the saturation absorption signal.

A lens placed just outside one of the view ports of the vacuum chamber served to collect the fluorescence emission from the cloud and focus it onto a femtowatt detector. A constant current was passed through the getter source throughout the experiment.

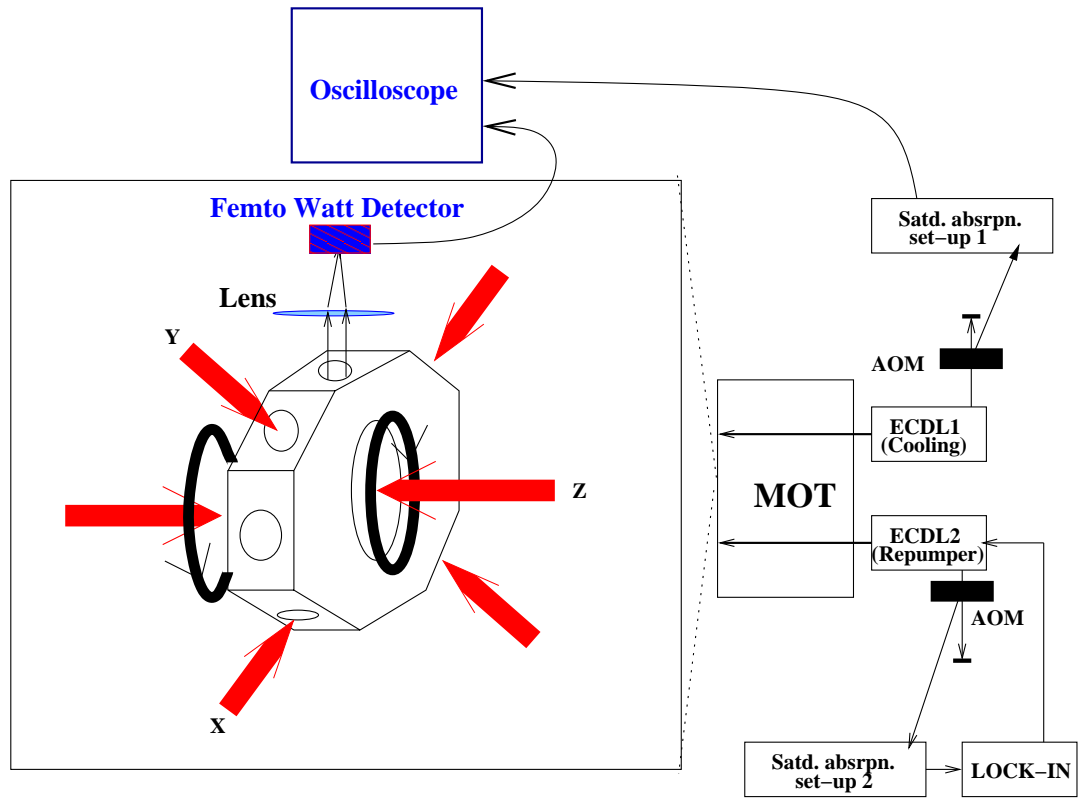


Figure 3.2: A schematic experimental set-up. AOM: acousto-optic-modulator

3.3 Observations

Figures 3.4 to 3.6 show the fluorescence data when the cooling beam frequency is ramped down (δ_c becoming more negative) and ramped up (δ_c becoming less negative) for three different values of the detuning δ_r of the repumper namely, -9.8 MHz (figure 3.4), 0 (figure 3.5) and +9.8 MHz (figure 3.6). Ramp period was kept fixed at 33.3 s in the above cases.

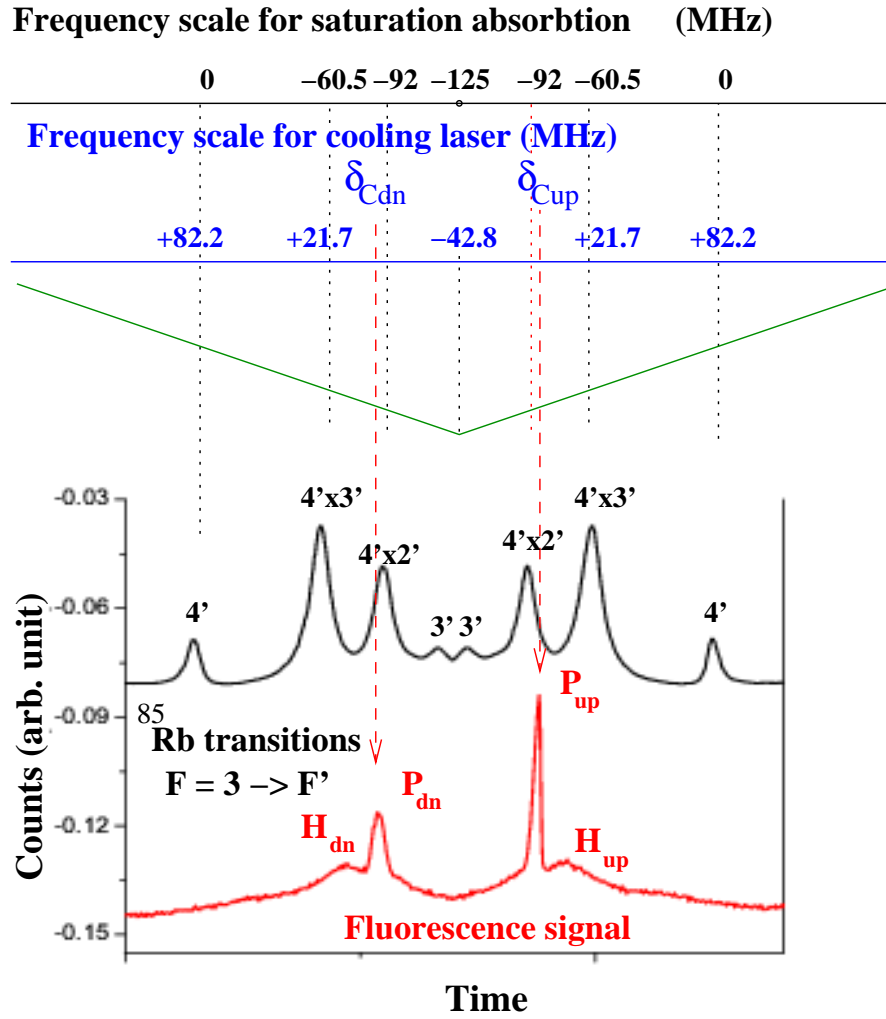


Figure 3.3: Lower trace (red) gives the fluorescence signal recorded as a function of time as the cooling laser is ramped down and then ramped up. The upper trace is the saturation absorption signal used as a frequency reference. The green line is the frequency ramp. The top line gives the detuning of light in the saturation absorption. The blue line gives the detuning of the cooling laser beams going to the MOT. The detuning is measured from the $3 \rightarrow 4'$ transition. δ_r for this run is -2 MHz.

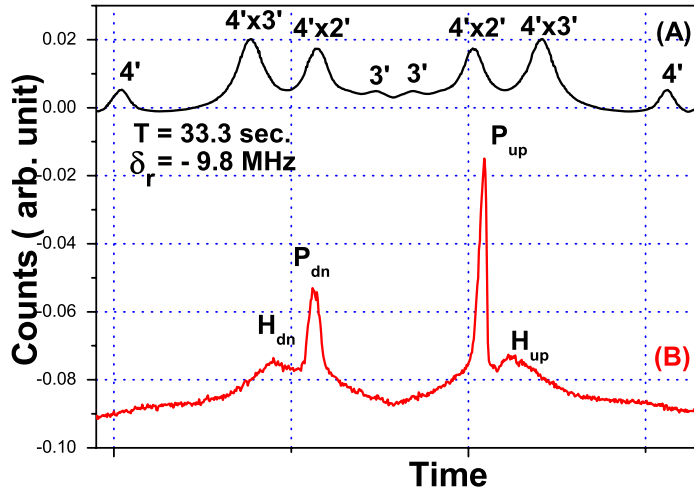


Figure 3.4: Oscilloscope traces of (A) saturation absorption signal of cooling laser, giving its instantaneous frequency, and (B) fluorescence intensity recorded by the femtowatt detector (ramp period 33.3 s, $\delta_r = -9.8$ MHz). The left half of the signal is due to the ramping of the detuning down (δ_c becomes more negative) and the right part due to the ramping of the detuning up (δ_c becomes less negative).

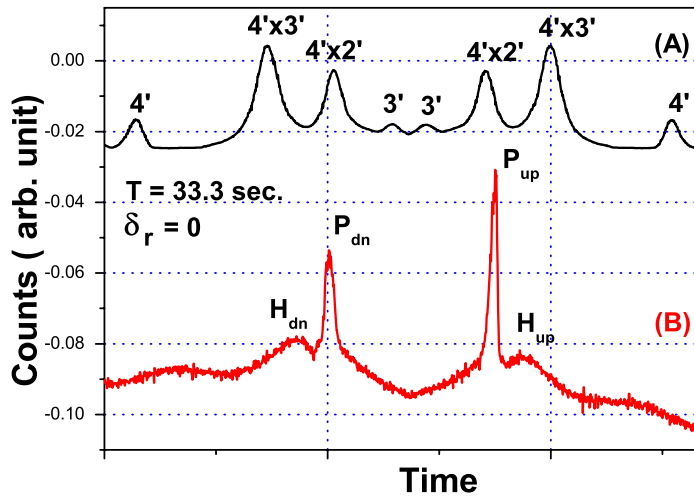


Figure 3.5: Oscilloscope traces of (A) saturation absorption signal of cooling laser, giving its instantaneous frequency, and (B) fluorescence intensity recorded by the femtowatt detector (ramp period 33.3 s, $\delta_r = 0$).

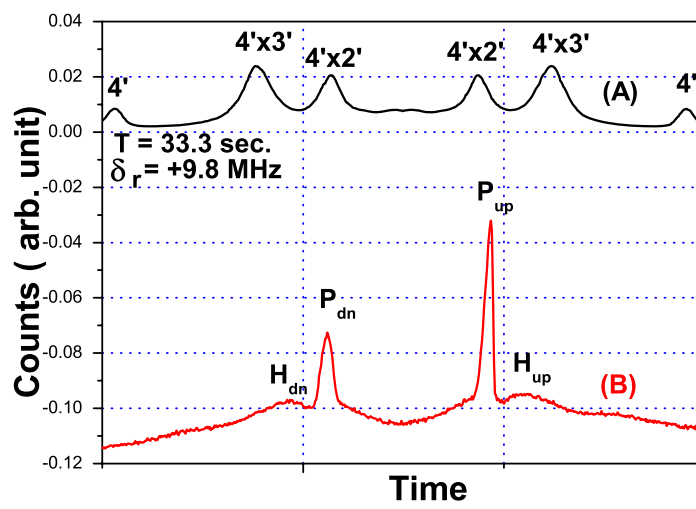


Figure 3.6: Oscilloscope traces of (A) saturation absorption signal of cooling laser, giving its instantaneous frequency, and (B) fluorescence intensity recorded by the femtowatt detector (ramp rate, period 33.3 s, $\delta_r = +9.8$ MHz).

The fluorescence intensity shows a maximum once during the downward ramp and once during the upward ramp. These peaks are called P_{dn} and P_{up} respectively. They occur at different values of the detuning δ_c . Figures 3.7 to 3.12 give the data for a fixed detuning of δ_r but different ramp periods.

A prominent feature is that the fluorescence peaks are of unequal intensities. For example in figure 3.7 which corresponds to $\delta_r = -9.8$ MHz and ramp period 10 s (ie., rate of change of frequency 31 MHz/s), the relative heights above the background of the peaks P_{dn} and P_{up} , that is, I_{dn}/I_{up} is approximately 0.32. For the same δ_r , but at higher ramp period of 100s (ie rate of change of frequency 3.1 MHz/s, figure 3.7) the ratio of the two peaks is approximately 0.51. As the ramp period decreases (ie rate of change of detuning is increased) the relative peak height I_{dn}/I_{up} decreases. This is clearly seen in all the figures from 3.7 to 3.12. At fast ramp rates (105 MHz/s or more), the peak P_{dn} degrades and itself appears as a mere hump (see figure 3.12, $T = 3.3$ s.). When ramped slowly, yet another hump (H_{2up} , H_{2dn}) appears as seen in figure 3.10 for $T = 125$ s.

We concentrate mainly on the major peaks P. From the figures 3.7 to 3.12 we find the detunings δ_{up}/Γ and δ_{dn}/Γ at which the peaks P_{up} and P_{dn} occur, their widths at half maximum $(FWHM)_{up}/\Gamma$, $(FWHM)_{dn}/\Gamma$ and the ratio $\rho = I_{dn}/I_{up}$. These data are summarized in Tables 3.1 to 3.6.

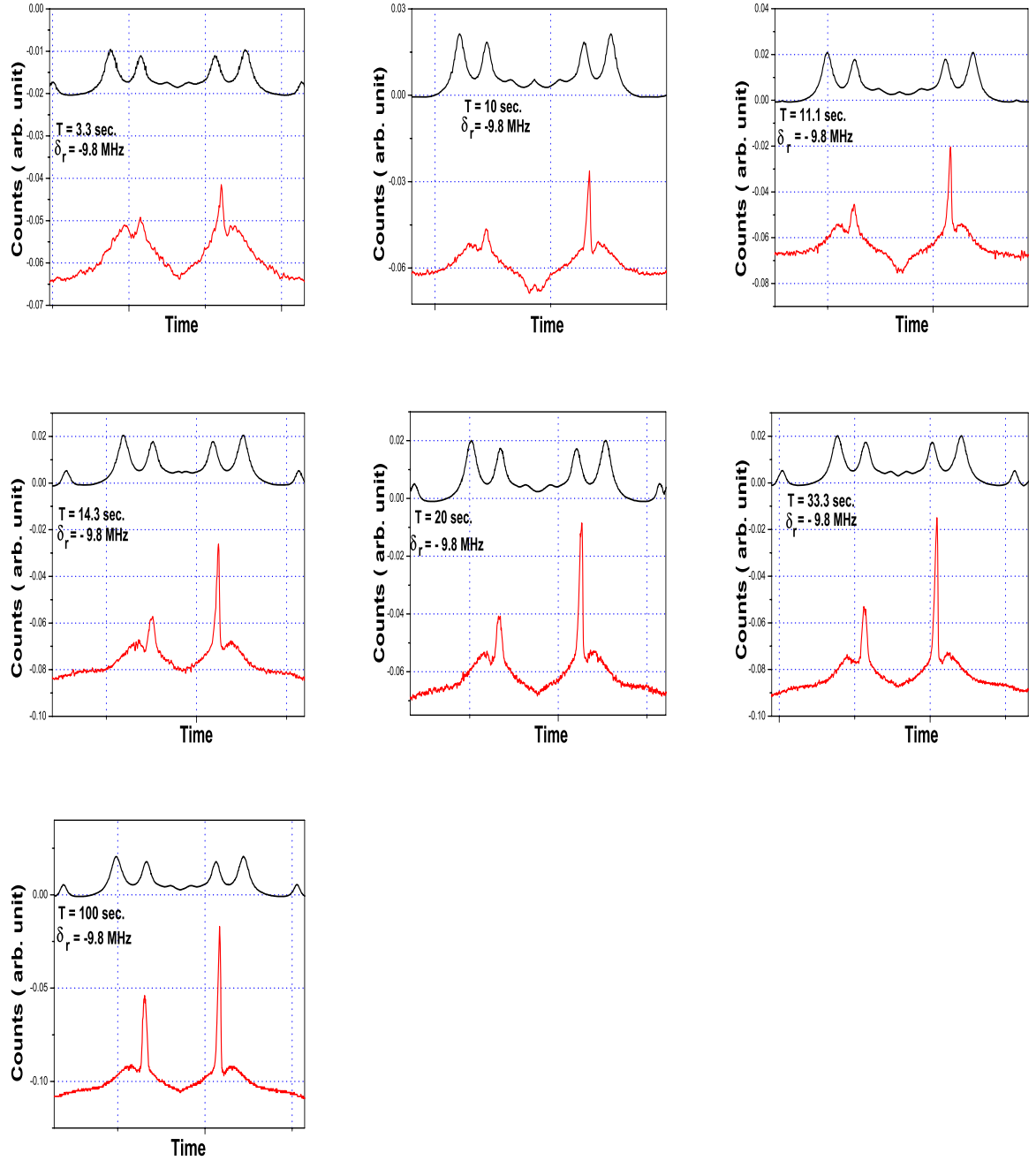


Figure 3.7: Oscilloscope traces of saturation absorption of cooling laser (upper trace) and the fluorescence signal from the MOT (lower trace) for various ramp rates of the cooling laser, when the repumper detuning $\delta_r = -9.8$ MHz.

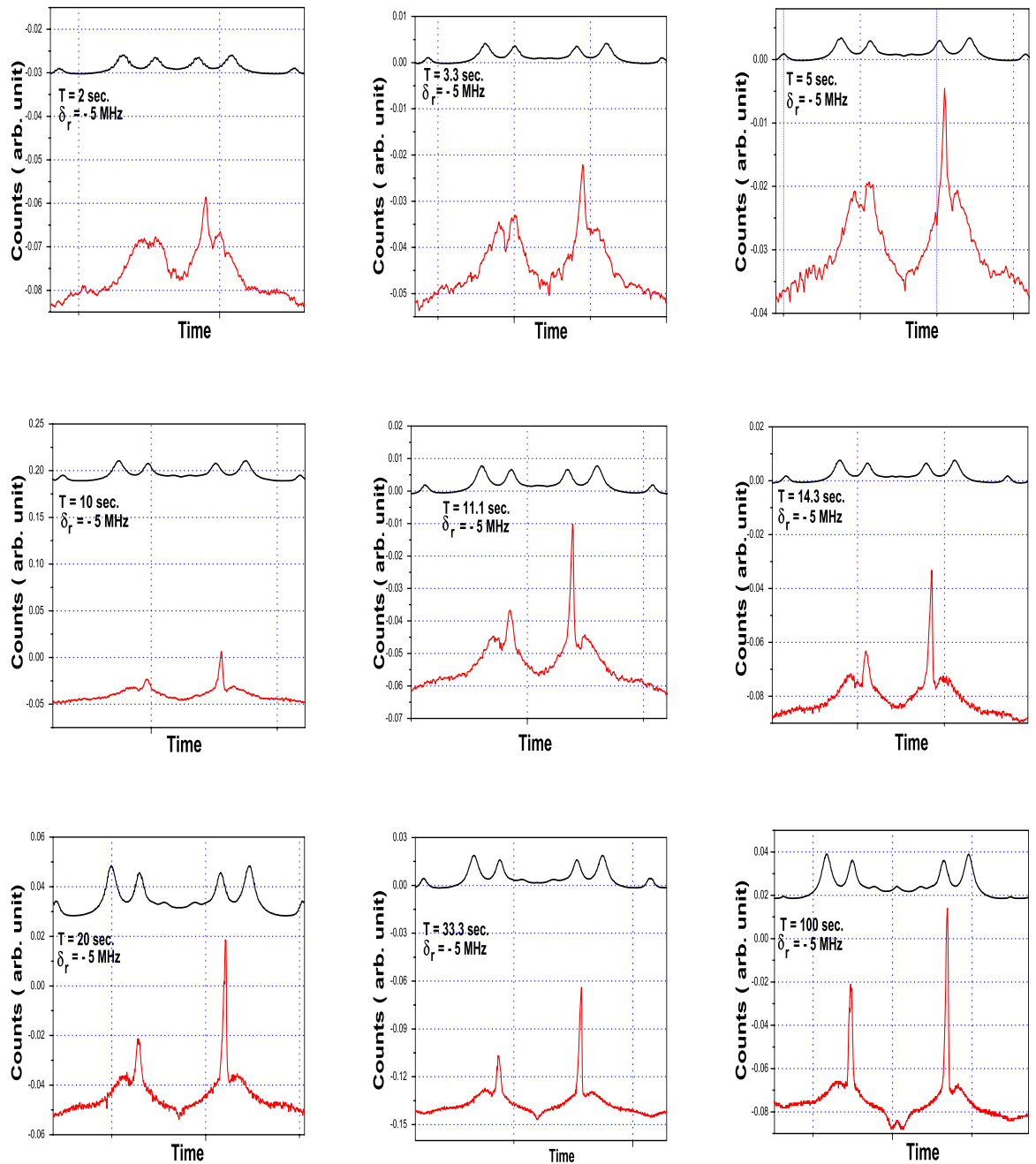


Figure 3.8: Oscilloscope traces of saturation absorption of cooling laser (upper trace) and the fluorescence signal from the MOT (lower trace) for various ramp rates of the cooling laser, when the repumper detuning $\delta_r = -5$ MHz.

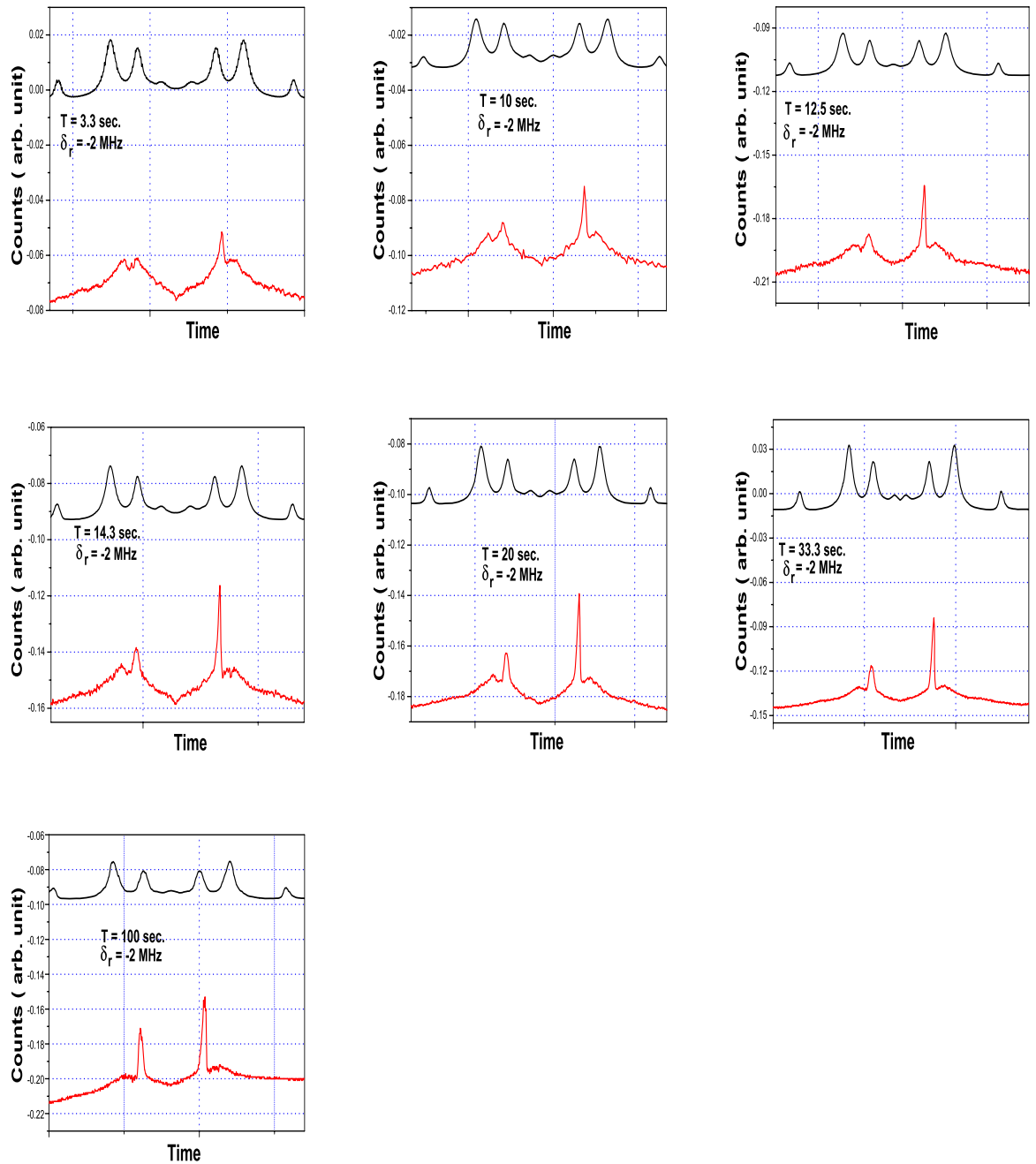


Figure 3.9: Oscilloscope traces of saturation absorption of cooling laser (upper trace) and the fluorescence signal from the MOT (lower trace) for various ramp rates of the cooling laser, when the repumper detuning $\delta_r = -2$ MHz.

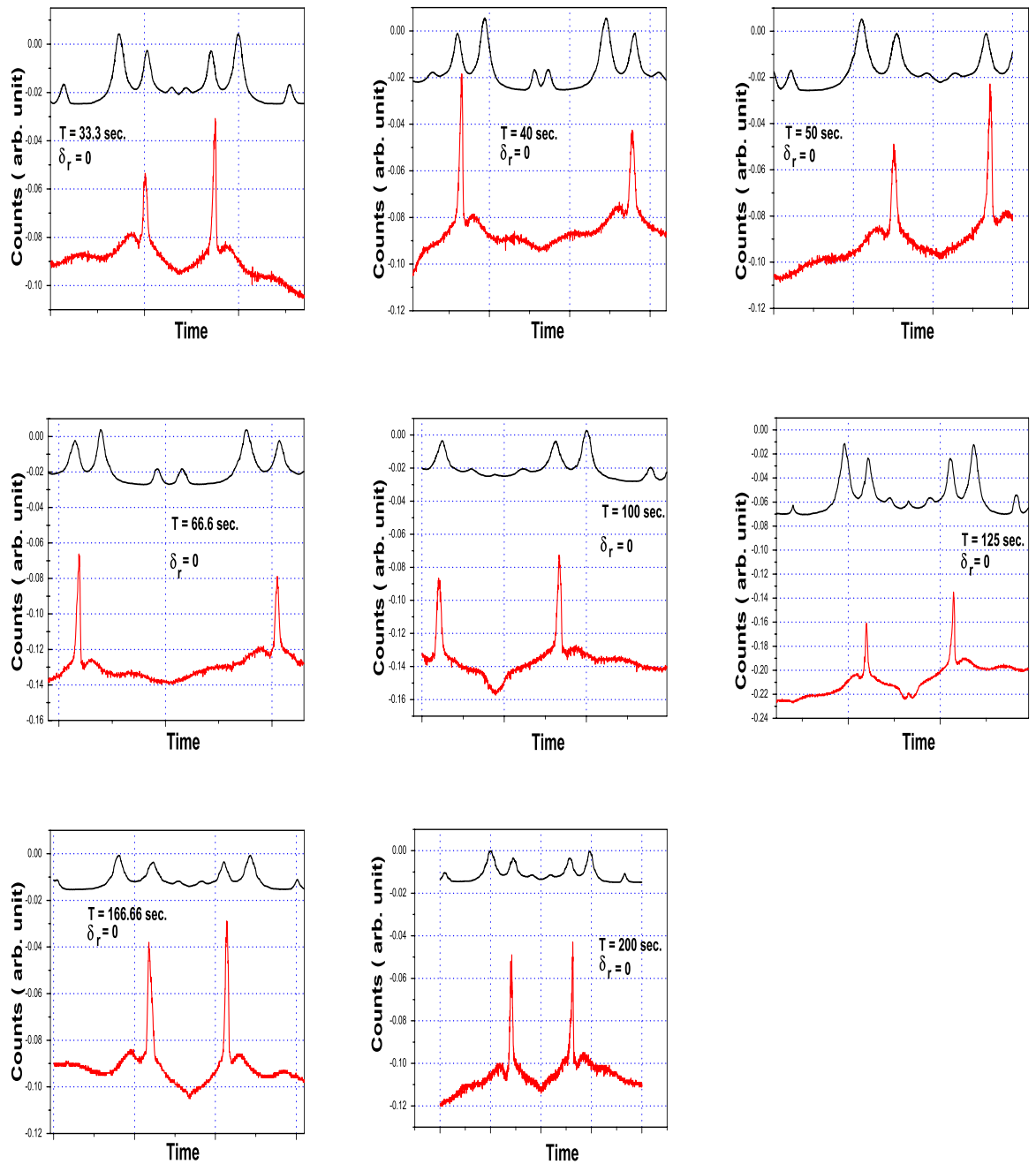


Figure 3.10: Oscilloscope traces of saturation absorption of cooling laser (upper trace) and the fluorescence signal from the MOT (lower trace) for various ramp rates of the cooling laser, when the repumper detuning $\delta_r = 0$ MHz.

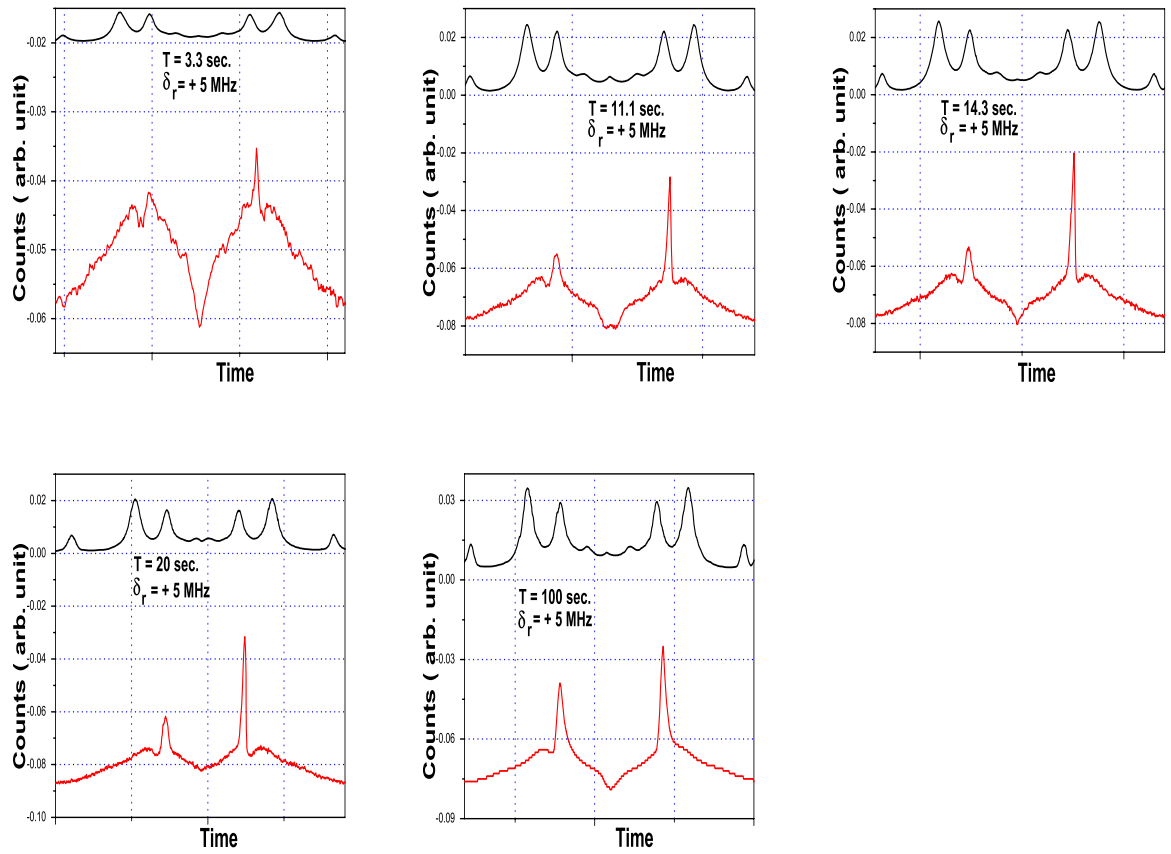


Figure 3.11: Oscilloscope traces of saturation absorption of cooling laser (upper trace) and the fluorescence signal from the MOT (lower trace) for various ramp rates of the cooling laser, when the repumper detuning $\delta_r = +5 \text{ MHz}$.

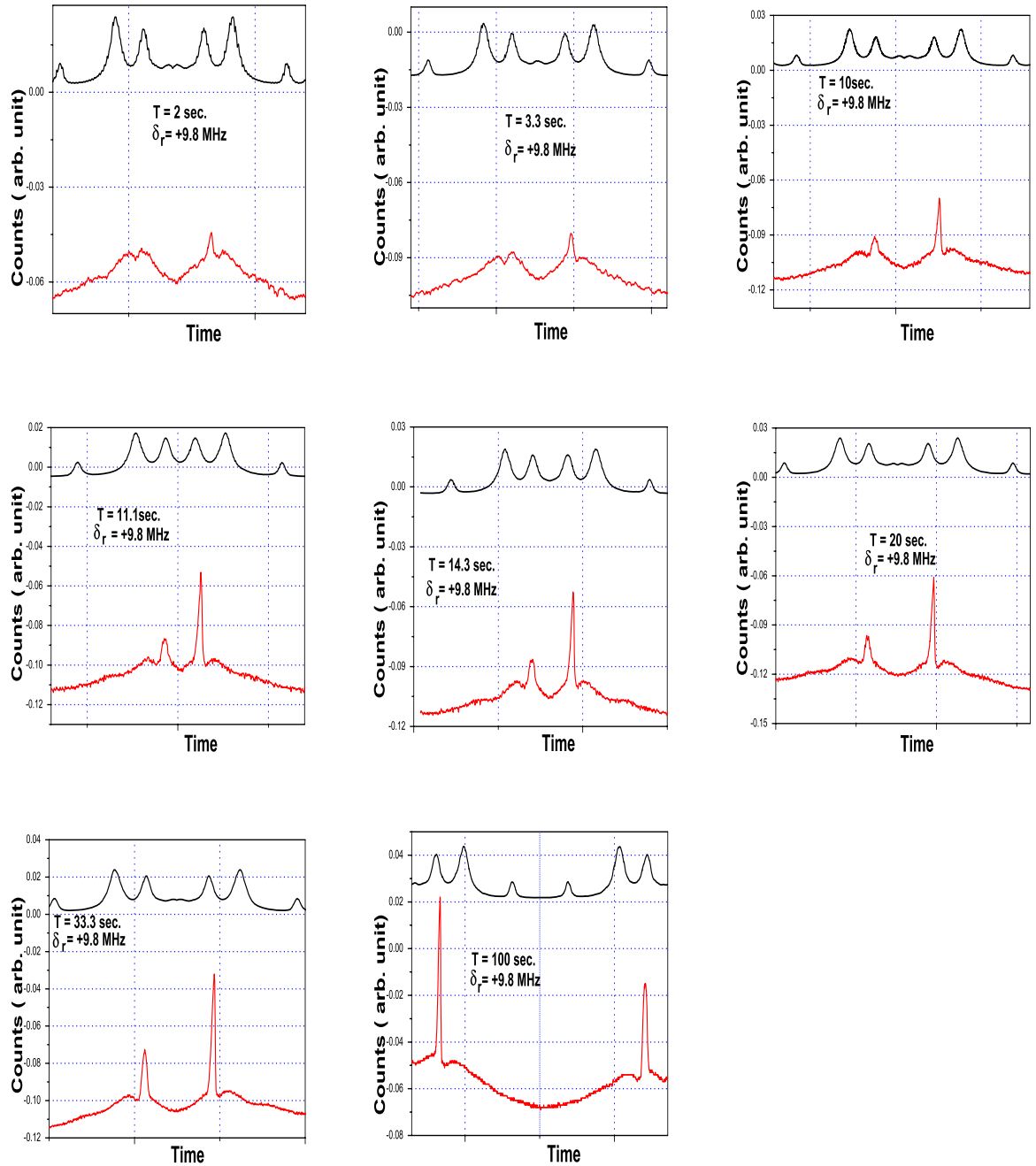


Figure 3.12: Oscilloscope traces of saturation absorption of cooling laser (upper trace) and the fluorescence signal from the MOT (lower trace) for various ramp rates of the cooling laser, when the repumper detuning $\delta_r = +9.8$ MHz.

Ramp period (sec)	(δ_{up}/Γ)	(δ_{dn}/Γ)	$(FWHM)_{up}/\Gamma$	$(FWHM)_{dn}/\Gamma$	$\rho = I_{dn}/I_{up}$
100	-0.96	-1.28	0.62	0.8176	0.513
33.3	-0.8	-1.42	0.69	1.05	0.381
20	-0.71	-1.40	0.75	1.14	0.329
14.3	-0.63	-1.47	0.772	1.193	0.383
11.1	-0.63	-1.43	0.592	1.11	0.363
10	-0.61	-1.3	0.685	1.22	0.317
3.3	-0.48	-1.5	0.77	1.038	0.592

Table 3.1: Repumper detuning $\delta_r = -9.8$ MHz, FWHM is the width of the peak.

Ramp period (sec)	(δ_{up}/Γ)	(δ_{dn}/Γ)	$(FWHM)_{up}/\Gamma$	$(FWHM)_{dn}/\Gamma$	$\rho = I_{dn}/I_{up}$
100	-0.85	-1.3	0.69	0.8522	0.570
33.3	-0.723	-1.42	0.7	0.898	0.330
20	-0.663	-1.40	0.68	1.096	0.449
14.3	-0.667	-1.31	0.644	1.05	0.317
11.11	-0.624	-1.53	0.64	1.24	0.302
10.0	-0.65	-1.51	0.766	1.31	0.276
5	-0.54	-1.63	0.6564	0.91	0.337
3.3	-0.45	-1.364	0.92	1.48	0.406
2	-0.54	-1.05	0.875	2.33	0.441

Table 3.2: Repumper detuning $\delta_r = -5$ MHz, FWHM is the width of the peak.

Ramp period (sec)	(δ_{up}/Γ)	(δ_{dn}/Γ)	$(FWHM)_{up}/\Gamma$	$(FWHM)_{dn}/\Gamma$	$\rho = I_{dn}/I_{up}$
100	-0.81	-1.183	0.772	0.85	0.660
33.3	-0.583	-1.375	0.75	1.034	0.3384
20	-0.66	-1.371	0.73	1.181	0.356
14.3	-0.48	-1.46	0.623	1.25	0.263
12.5	-0.69	-1.43	0.651	1.235	0.282
10	-0.583	-1.37	0.84	1.313	0.277
3.3	-0.540	-1.56	0.73	0.96	0.1414

Table 3.3: Repumper detuning $\delta_r = -2$ MHz, FWHM is the width of the peak.

Ramp period (sec)	(δ_{up}/Γ)	(δ_{dn}/Γ)	$(FWHM)_{up}/\Gamma$	$(FWHM)_{dn}/\Gamma$	$\rho = I_{dn}/I_{up}$
200	-0.913	-1.186	0.48	0.6972	0.893
166.6	-1.03	-0.918	0.736	0.639	0.845
125	-0.92	-1.264	0.5	0.5	0.779
100	-1.05	-1.102	0.71	0.82	0.766
66.16	-0.83	-1.3	1.05	0.6	0.714
50	-1.185	-1.113	0.622	0.78	0.649
40	-0.885	-1.14	0.5924	0.9	0.592
33.3	-0.88	-1.31	0.611	0.82	0.522

Table 3.4: Repumper detuning $\delta_r = 0$ MHz, FWHM is the width of the peak.

Ramp period (sec)	(δ_{up}/Γ)	(δ_{dn}/Γ)	$(FWHM)_{up}/\Gamma$	$(FWHM)_{dn}/\Gamma$	$\rho = I_{dn}/I_{up}$
100	-0.622	-1.541	1.011	1.06	0.625
33.3	-0.672	-1.337	0.74	1.035	0.323
20	-0.679	-1.44	0.6	1.088	0.315
14.3	-0.600	-1.283	0.69	1.05	0.261
11.1	-0.583	-1.52	0.7	1.25	0.298
3.3	-0.552	-1.47	0.62	1.43	0.412

Table 3.5: Repumper detuning $\delta_r = +5$ MHz, FWHM is the width of the peak.

Ramp period (sec)	(δ_{up}/Γ)	(δ_{dn}/Γ)	$(FWHM)_{up}/\Gamma$	$(FWHM)_{dn}/\Gamma$	$\rho = I_{dn}/I_{up}$
33.3	-0.70	-1.411	0.69	1.035	0.354
20.0	-0.72	-1.454	0.6	0.954	0.285
14.3	-0.76	-1.471	0.59	1.13	0.307
11.1	-0.62	-1.391	0.66	1.02	0.2742
10	-0.59	-1.296	0.71	1.11	0.304
3.3	-0.39	-1.5	0.69	0.83	0.22

Table 3.6: Repumper detuning $\delta_r = +9.8$ MHz, FWHM is the width of the peak.

From a perusal of Tables 3.1 to 3.6 and figures 3.7 to 3.12 we can draw the following conclusions:

1. The detuning at which the peaks occur changes with the ramp period. As the ramp period is decreased P_{up} moves towards δ_{up}/Γ tending to 0, while P_{dn} appears to move generally more towards the red detuning though this is not always the case.
2. The full width at half maximum of P_{up} is always less than Γ while the full width at half maximum of P_{dn} generally becomes very broad at very low ramp periods(very fast ramping).
3. The ratio of the peak intensities $\rho = I_{dn}/I_{up}$ increases as the ramp period increases and approaches the value 1 for very long ramp periods.
4. For a given ramp period the ratio ρ is a maximum when the repumper detuning is zero. ρ decreases as the repumper detuning is changed from zero.

3.4 Analysis and Discussions

One would expect that the fluorescence depends on the instantaneous number of atoms in the MOT, which in turn depends on the instantaneous detuning of the cooling laser. Hence, it should not matter whether a particular detuning has been approached from the red side or the blue side. However, the fluorescence data very clearly indicate that this is not the case. For example, from figure 3.7 ($T= 100s$), $I_{up} > I_{dn}$, that is the height of the peak when approached from the red side is nearly two times more than that when approached from the blue side. It is thus clear, that it is not merely the instantaneous detuning that governs the fluorescence, but also the path followed, or the “history” that is important. To understand this, let us examine the processes occurring in the trap.

There are two timescales relevant to a MOT. The first is the lifetime of the atom in the excited state which is ≈ 100 ns. Repeated absorption-emission cycles extract energy from the atoms, which, over several milliseconds, are cooled enough to be trapped. The other one

is the lifetime of the atoms in the MOT which is in the range 0.1 s to even 100 s depending upon the pressure. If the detuning of the cooling beam is ramped slowly adiabaticity can be ensured; that is, the loading rate and the lifetime in the trap may be assumed to adjust to the instantaneous detuning of the laser beam. The fastest speed at which the detuning was ramped was 155 MHz/s. So to cover the natural line-width of 6 MHz at this ramp rate the time involved will be approximately 40 ms. On the otherhand the cooling and trapping of the atom take place in a time of less than 10 ms. So this assumption can be taken to be reasonably valid even at the fastest ramp rate. The number of atoms in the trap will be determined by the balance between the two opposing processes - collection into and exit from the trap.

Thus, the cold cloud formed in a MOT is in a dynamic equilibrium, with atoms being continuously loaded into the cloud by cooling and capture, and atoms escaping from the cloud due to collisions. The number of atoms follows the rate equation

$$dN/dt = R_L - N/\tau \quad (3.1)$$

where N is the number of atoms in the trap, R_L the loading rate of atoms to the MOT from the background vapor, τ is the lifetime of the atom in the MOT. At room temperature Rb atoms have a most probable velocity around 250 m/s. Their velocity distribution follows a Maxwell-Boltzmann distribution and the velocity classes near the low velocity tail of the distribution curve can be slowed down after undergoing repeated cooling-cycle transitions and trapped in the MOT. The loading rate, R_L depends on a capture velocity, V_C of the atom. V_C is the highest velocity of entrance of an atom that is stopped in a maximum distance equal R_c , called the capture radius. R_c will be equal to the size of the molasses region where the optical beams overlap [1]. V_C depends on the radius of capture, the intensity I , the detuning δ_c of the cooling beams, and the magnetic field gradient in the MOT.

V_C was estimated as a function of the detuning (see figure 3.13) by simulating the deceleration of an atom that continuously scatters light from the beams propagating co- and counter- to its direction of motion. This was done as follows:

For simplicity, a 1-D case was considered with the molasses region extending from $-R_c$

to $+R_c$ about the center. To know the capture velocity for certain MOT parameters we allow atoms with a range of initial velocities v_i to enter the capture region at R_c . The force acting on the atom in the MOT is calculated using the formula

$$\begin{aligned} \mathbf{F} &= \hbar \mathbf{k} \Gamma \left[\frac{I/I_s}{1 + I/I_s + (4/\Gamma^2)(\delta_c + kv - (\mu/\hbar)(dB/dz)z)^2} \right] \\ &+ \hbar \mathbf{k} \Gamma \left[\frac{I/I_s}{1 + I/I_s + (4/\Gamma^2)(\delta_c - kv + (\mu/\hbar)(dB/dz)z)^2} \right] \quad (3.2) \\ &\equiv \mathbf{F}_+ + \mathbf{F}_- \quad (3.3) \end{aligned}$$

where \mathbf{F}_+ and \mathbf{F}_- include the damping forces due to the Doppler shift ($\pm kv$) in the light beam and the restoring forces from the Zeeman shift due to the field gradient ($\pm \mu(dB/dz)z$). In the above equation \mathbf{k} is the wave vector, I and I_s are intensity and the saturation intensity of the cooling laser beam respectively, μ the effective magnetic moment for the cooling transition, dB/dz the magnetic field gradient. For our simulation we have chosen $(I/I_s) = 1$; $\mu = \mu_B$ one Bohr magneton and $dB/dz = 1000$ G/m, $R_c = 2$ mm. Inside the MOT the atom experiences deceleration

$$\mathbf{f} = \mathbf{F}/m \quad (3.4)$$

Simulation consists of tracking the position and the velocity of an atom at intervals of $10\mu s$. The atom enters with a velocity v_i into the MOT. After a time τ the velocity v

$$v = v_i + f\tau \quad (3.5)$$

and its position z

$$z = R_c - (v_i\tau + 0.5f\tau^2) \quad (3.6)$$

As the atom moves into the MOT z will decrease from a value R_c at $t=0$. This calculation is repeated sequentially till either v becomes zero within the MOT, or z becomes $< -R_c$ (ie the atom has come out of the capture region). If v becomes zero at z ($R_c > z > -R_c$) the atom is captured in the MOT; otherwise not. We have done the simulations using Matlab.

In the initial calculation the magnetic field gradient was taken to be zero. This means we are calculating the capture velocity for the optical molasses. V_c as a function of δ/Γ is shown

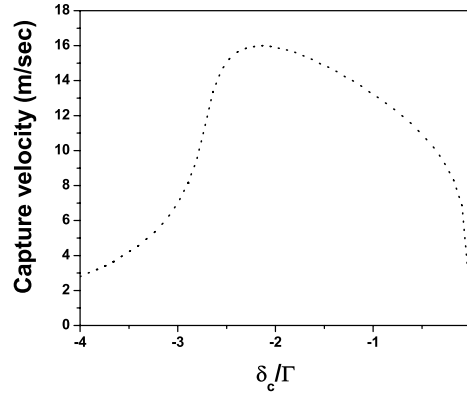


Figure 3.13: Variation of the capture velocity with the detuning of the cooling laser in an optical molasses

in figure 3.13. Starting from zero at zero detuning, V_C increases rapidly, with detuning till δ/Γ is approximately -0.2. Thereafter it increases more slowly till $\delta/\Gamma \approx -2.2$, at which point it reaches its maximum value of 16m/s. Further increase in detuning results in a steep fall in V_C which levels off at $V_C \approx 3$ m/s and δ/Γ is ≈ -4 .

Next the same calculation was repeated including the effect of magnetic field. The trajectory of an atom in phase space is given in figure 3.14.

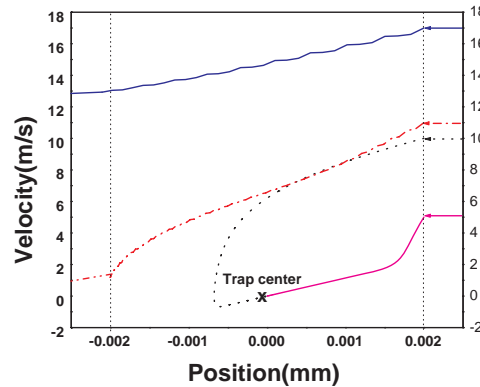


Figure 3.14: Numerical simulation of the capture process in one-dimension of the Magneto-Optical-Trap. Different lines are the trajectories of the Rb atoms inside the MOT region with different initial velocities. For high velocities (blue and red curves) the atom escapes from the capture region ie z become less than $-R_c$. For low enough velocities (dotted and pink curves) the atoms are collected in the center of the trap and remain trapped.

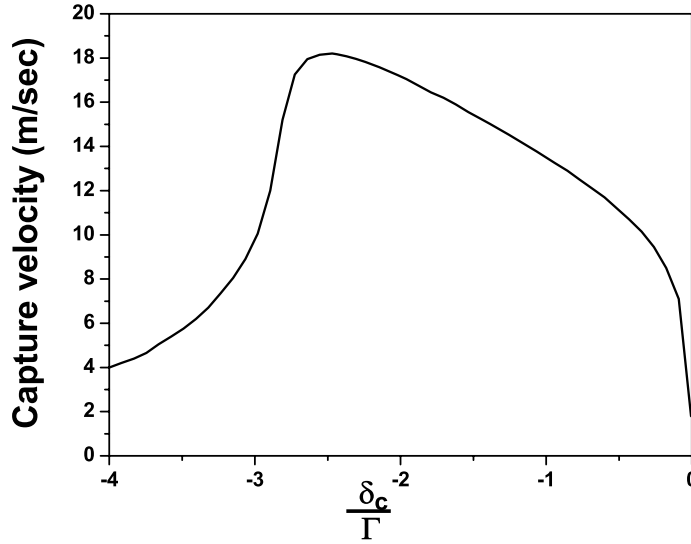


Figure 3.15: Variation of the capture velocity with the detuning of the cooling laser in a MOT. For simulation we have taken trapping field gradient 1000 G/m, $I/I_s = 1$, radius of the MOT = 2 mm.

Figure 3.15 gives V_C as a function of detuning. The shape of the curve is essentially the same as in figure 3.13. V_C rises rapidly from 0 at resonance to about 7 m/s at -0.2Γ , and continues to rise, but at slower rate, reaching the maximum value of about 18 m/s for detuning of about -2.6 MHz. Thereafter, V_C falls rapidly with detuning to about 8 m/s for a detuning of -2.6Γ . At large detunings, the descent continues, but at a slower rate. A notable difference however is that the V_C value at any detuning is larger in the presence of a magnetic field than without a field.

It is clear that the detuning of the cooling laser determines to a large extent, the capability of the beam to cool moving atoms. At red detunings of -2.6Γ of the cooling beam, atoms moving as fast as 18 m/s can be brought to a halt. Thus, a cloud formed with the cooling beam held at -2.6Γ is expected to have the maximum number of atoms.

Having obtained V_C , the kinetic theory of gases is used to calculate the loading rate R_L

(atomic flux into the MOT), using the formula [2]

$$R_L = (\bar{v}n/5)(V_C/\bar{v})^4 \quad (3.7)$$

where \bar{v} is the average speed of atoms at room temperature and n is the number density of atoms [1]. The effect of various parameters like capture radius, intensity of the cooling beams, magnetic field gradients have been studied. The results of calculations are plotted in figure 3.16.

In our simulation, we estimate the loading rates as a function of δ_c/Γ , varying from 0 to -4, where Γ is the natural linewidth of the cooling transition, and is $2\pi \times 6$ MHz. The general feature of the loading curves, as the detuning shifts to the red from zero, is a gradual rise to a peak value followed first by a rapid decay, and then by an asymptotic approach to zero. As the capture radius is increased from 1 mm to 5 mm (figure 3.16 (Top)), the loading rate peaks at larger detunings. This is expected because as the cooling beams become wider in extent, they can capture atoms further away from the centre. As the distance over which slowing can occur increases, the capture velocity increases and the loading rate as well.

Figure 3.16 (Center) shows the dependence of the loading rate on the intensity of the cooling beams as the latter is increased to its saturation value from one tenth the value. The basic shape of the loading curve remains the same. The curve broadens with intensity, and the peak rate of loading is obtained at larger detunings.

Figure 3.16 (Bottom) shows that doubling the magnetic field gradient has a very slight effect on the loading curve. We next examine the lifetime τ of the atoms in the trap. In a MOT the atoms execute a damped harmonic oscillation. The force constant κ of the harmonic potential in the MOT due to the quadrupolar coils is

$$\kappa = -16[(\delta/\Gamma)/\{1 + 2(I/I_s) + 4(\delta/\Gamma)^2\}^2](\mu/\hbar)(dB/dx)(\hbar k). \quad (3.8)$$

where μ is the magnetic moment of the atom in the ground state of the cooling transition [3], and k is the wave vector of the laser beam. Atoms will be trapped as long as their potential energy in the trap exceeds their kinetic energy. Thus, the escape velocity may be estimated as [3]

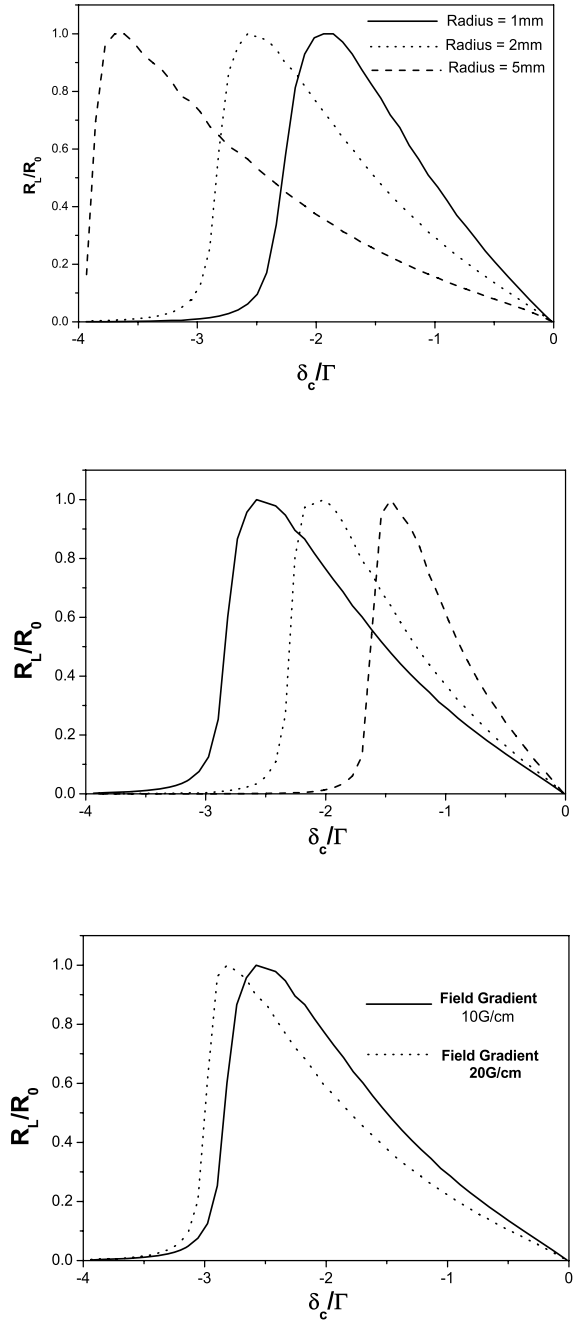


Figure 3.16: Normalized loading rate R_L/R_0 as a function of detuning for ^{85}Rb for (Top) different capture radii R_c , ($R_c = 1$ mm (solid line), 2 mm (dotted line) and 5 mm (dashed line)) taking $I/I_s = 1$; $\text{dB}/\text{dz} = 10$ Gauss/cm, (Center) different intensities of the cooling laser I/I_s ; ($I/I_s = 0.1$ (dashed line), $I/I_s = 0.4$ (dotted line), 1 (solid line)) taking $\text{dB}/\text{dz} = 10$ Gauss/cm, $R_c = 2$ mm, (Bottom) different trapping field gradient dB/dz ; taking $R_c = 2$ mm, $I/I_s = 1$.

$$mV_{esc}^2 = \kappa R^2 \quad (3.9)$$

where R is the trap radius. Steane et al [1] have pointed out that the life time will be proportional to V_{esc}^η . η is $2/3$ if the collisions leading to the escape are between the atoms, one of which is in the ground state and the other in the excited state whereas η is $1/3$ if both the colliding atoms are in the ground state. In the first case the interaction is van der Waals in nature, whereas in the latter case it is resonant dipole-dipole interaction. Therefore, lifetime τ depends on the detuning as (from equation 3.8)

$$\tau = \tau_0 \{ [(-\delta_c/\Gamma)(I/I_s)]^{1/2} / [1 + 2(I/I_s) + 4(\delta_c/\Gamma)^2] \}^\eta \quad (3.10)$$

where the parameter τ_0 depends on the trap radius, the effective magnetic moment, the magnetic field gradient and the pressure in the MOT. As seen from the above equation, τ/τ_0 depends only on the detuning and the intensity of the cooling beam. This has been calculated as a function of δ/Γ and shown in figure (3.17) for two values of η . As there are very few atoms trapped in the excited state, all further calculations assume $\eta = 1/3$. Also, at extremely low pressure in the MOT collisions with background atoms other than Rb are rare.

So far we have obtained the functional variation of both the loading rate and the decay rate, with the detuning. Next, we estimate the number of atoms in the trap and fluorescence intensity as a function of detuning, for different ramp rates. One may expect that the fluorescence intensity will be a maximum when the number of atoms in the trap is maximum. However, interestingly, our experimental results (and also our analysis) show that this is not the case.

Using the variable $N' = N/R_0\tau_0$, and $t' = t/\tau_0$, we may write the rate equation 3.1 for the number of atoms in dimensionless form as

$$dN'/dt' = R/R_0 - N'/(t'/\tau_0) \quad (3.11)$$

We assume the cooling laser is ramped from $+4\Gamma$, through zero, to -4Γ and back, the instan-

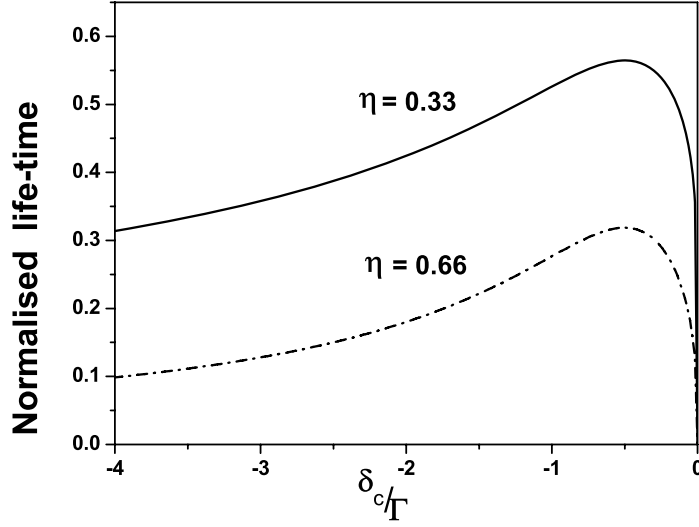


Figure 3.17: Normalized lifetime as a function of (δ_c/Γ) for $\eta = 1/3$ and $\eta = 2/3$.

taneous detuning can be written as

$$\delta_c(t)/\Gamma = +4 - 16(t/T) \quad 0 \leq t \leq T/2 \quad (3.12)$$

$$\delta_c(t)/\Gamma = +4 - 16(T - t)/T \quad T/2 \leq t \leq T \quad (3.13)$$

As no cooling or trapping takes place for blue detuned cooling beams, in the numerical simulation we solve the rate equation for the duration $T/4$ to $3T/4$ with the initial condition $N' = 0$ at $t = 0$. The fluorescence intensity at any time will be proportional to

$$I_{fl}(t) = N'(t)R_{sp} \quad (3.14)$$

where R_{sp} the spontaneous transition rate is given by

$$R_{sp} = \Gamma(I/I_s)/[1 + 2(I/I_s) + 4(\delta_c(t)/\Gamma)^2] \quad (3.15)$$

With the growth equation written in terms of dimensionless parameters, we obtain the fluorescent intensity as a function of δ_c/Γ , which is a function of t/τ_0 . In the manner outlined above, the number of atoms and the fluorescence intensity were calculated as a function of

δ_c/Γ for a range of time periods of the ramp, varying T/τ_0 from 1 to 200. A typical result is given in figure 3.18 and will be described now.

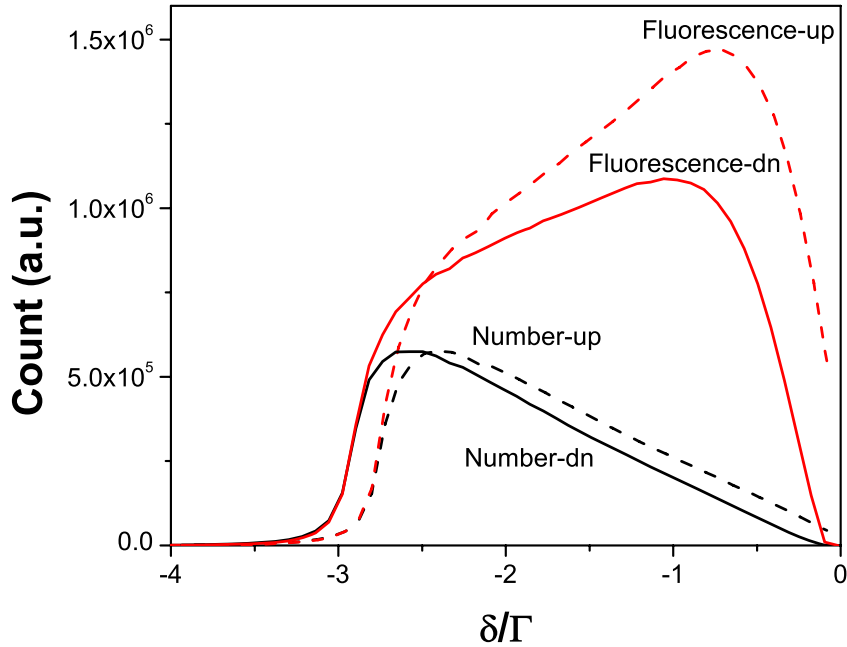


Figure 3.18: Theoretically estimated variation of number N' of atoms in the trap and the fluorescence intensity with detuning $\delta_c(t)/\Gamma$, while detuning ramped down and up from and to zero respectively.

When the detuning is varied from 0 to -4Γ (ramp down, solid curves), the number of atoms in the trap increases gradually, reaches a maximum at about -2.5Γ , and then falls rapidly. On the return path (ramp up from -4Γ to 0, dashed curve), the general shape of the curve is the same. The peak, however, occurs at a smaller detuning. The dependence of the fluorescent intensity on the detuning, however, is quite different from that of the population. On ramp down (solid curve), the intensity rises rapidly, reaching a maximum at detunings of about -1Γ , has a slow descent till about -2.5Γ and then falls off rapidly. During ramp up the general shape of the curve is overall the same, the fluorescence peak occurring at smaller detuning. The most striking feature, however, is that the peak intensity during upward ramp

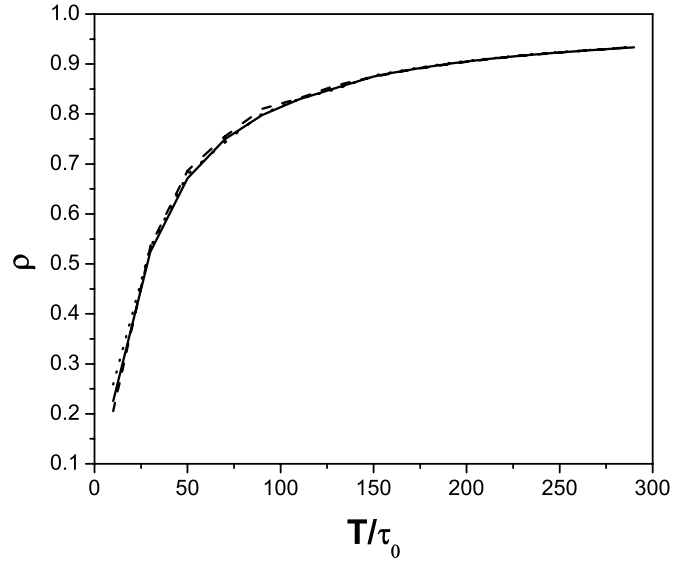


Figure 3.19: Theoretically estimated variation of asymmetry parameter ρ , as a function of T/τ_0 , for three different capture radii R_c (1 mm, 2 mm, 5 mm) of the MOT taking $I/I_s = 1$ and $dB/dz = 10$ Gauss/cm, all curves fall on top of each other.

is much larger than in the downward ramp. Thus, while the number of atoms is essentially the same for a given detuning, irrespective of whether the laser frequency has been ramped up or ramped down, the fluorescent intensity depends on whether a particular detuning has been approached from the red or the blue side. This is exactly what has been observed in our experiments. This distinction arises due to the strong dependence of R_{sp} on δ_c/Γ . The parameter $\rho = I_{dn}/I_{up}$ is small at fast ramp rates. As the ramp rate was slowed, ρ tended to 1 as shown in figure 3.19, obtained from our calculations. This same behavior is also seen in our experiments. We examined the dependence of the parameter ρ on the various MOT parameters like the capture radius (see figure 3.19), the intensity of the cooling beam (see figure 3.20), and the gradient of the magnetic field (see figure 3.21). The ρ vs T/τ_0 curve is remarkably robust and fairly insensitive to these three parameters over the entire range of their values found in typical MOTs even though the position of the fluorescence peaks, their widths, the number of atoms in a MOT etc. are fairly sensitive to the MOT parameters. How one can use ρ vs T/τ_0 curve to estimate the lifetime of the MOT will be discussed below.

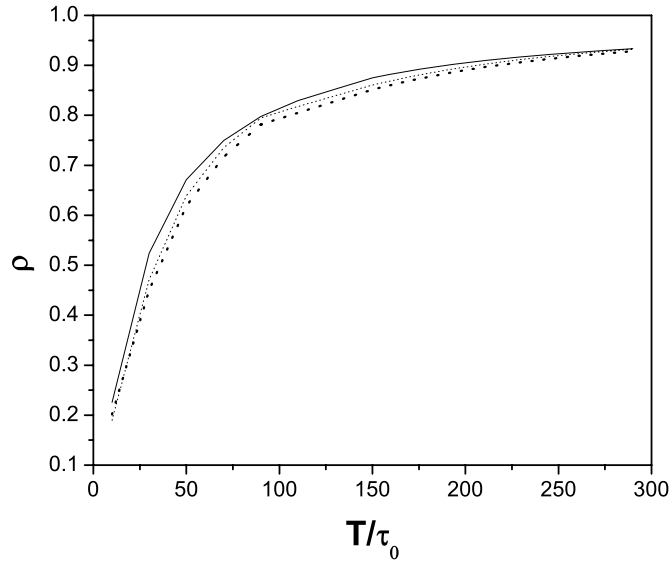


Figure 3.20: Variation of asymmetry parameter ρ , as a function of T/τ_0 , for three different I/I_s (0.1, 0.4, 1), taking the radius of the MOT 2 mm and $\text{dB}/\text{dz} = 10$ Gauss/cm.

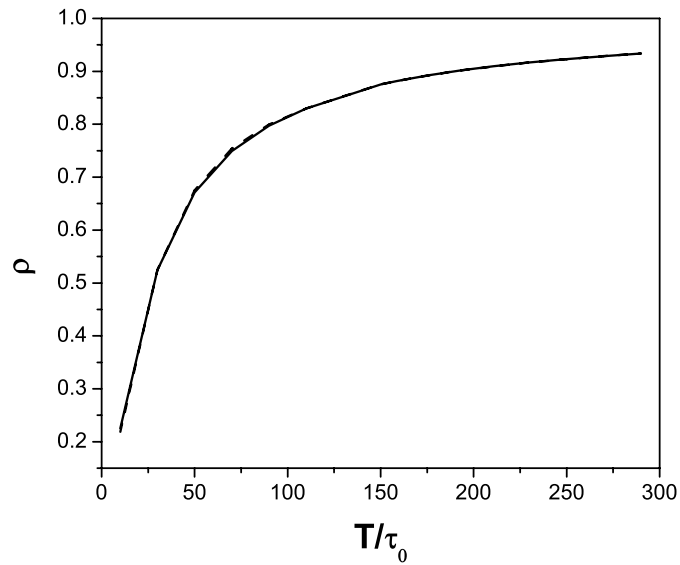


Figure 3.21: Variation of asymmetry parameter ρ , the ratio of the intensity of fluorescent peaks while ramping down to that while ramping up as a function of T/τ_0 , for two different magnetic field gradient (10 G/cm, 20 G/cm), taking the radius of the MOT 2 mm and $I/I_s = 1$.

Determination of lifetime: Fluorescence measurements had been carried out for different frequency ramp periods T , ranging from $T = 33.3$ s to 200 s (see Table 3.4). From these we obtained 8 different values of ρ . Using one of these values (that for the ramp period 66.16 s) we find from the curve 3.19 the value of T/τ_0 as 57.5. From this we estimate τ_0 to be 1.16 s. We have leastsquare fitted the ρ values for all the eight points adjusting the value of τ_0 around 1.16 s. We found the best fit for all the eight points with a value of $\tau_0 = 1.25$ s. Figure 3.22 shows a plot of the experimental ρ vs T/τ_0 . The error in measuring ρ arises from an estimation in the background and amounts to $\pm 3\%$ for these data. The data points

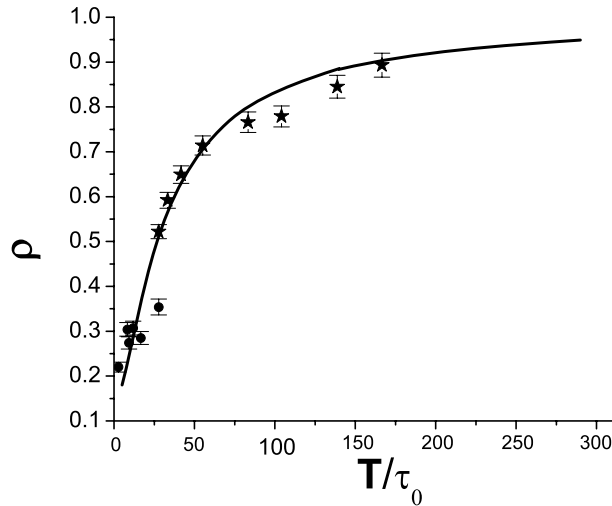


Figure 3.22: Theoretically estimated asymmetry parameter (solid line) as function of T/τ_0 for $\tau_0 = 1$, $\delta_c/\Gamma = 4.0$. The stars and full circles are experimentally observed values.

are shown as stars. The continuous curve is the calculated curve described earlier in fig 3.19. For another set of experiments for $T = 3$ s to 33 s carried out on a different day(see table 3.6) the points are plotted as circles on the same graph with the same value of τ_0 . We find the fit to these data points is also good. We calculate from τ_0 the lifetime τ for $\delta/\Gamma = 0.5$ using equation 3.10 as 0.7 s \pm 0.05 s. The lifetime determined is quite compatible with the value of pressure of 1×10^{-9} Torr in the MOT chamber. Thus the measurement of the ratio of peak intensities of the fluorescence peaks when the detuning is ramped will give information about the lifetime of the atoms in the trap. If ρ is measured with one ramp period, then one

can read off from the ρ curve (figure 3.19) the value of T/τ_0 appropriate to this value of ρ and then get the value of τ_0 . A check on this value can be made by measuring the value of ρ for another ramp period.

Usually, the lifetime of the trap is determined by switching off the atomic source and measuring the decay of the fluorescence of the trapped atoms as a function of time. If we are using a getter source it will take some time for the source to become cold. So Rb vapour will still be coming out of the source though in decreasing quantities. This will cause an error when the decay of fluorescence is measured. The method we have described above is a simple technique that neither requires switching off the source, nor measuring the rapid decay in fluorescence. It requires monitoring the fluorescent emission from the cold cloud as a function of the detuning of the cooling laser that is slowly ramped up and down.

To summarise, we have experimentally observed an asymmetry in the fluorescence intensity from a cold cloud in a MOT when the frequency of the cooling laser is ramped up or ramped down across the cooling transition. The observation is explained and an asymmetry parameter ρ is defined. A curve of ρ vs T/τ_0 is theoretically derived and experimentally verified. This curve is insensitive to various MOT parameters. From this the lifetime of the cloud can be estimated in a simple and non-destructive way.

Bibliography

- [1] A. M. Steane, M. Chowdhury, and C. J. Foot, Journal of Optical Society of America B **9**, 2142(1992).
- [2] Fundamentals of statistical and thermal physics, Federick Reif (McGraw-Hill, (1985)).
- [3] Laser Cooling and Trapping, H.J. Metcalf and P. van der Straten (Springer-Verlag New York, Inc. (1999)).